j. Global ocean carbon cycle—R. A. Feely, R. Wanninkhof, P. Landschützer, B. R. Carter, and J. A. Triñanes

1) Introduction

The oceans play a major role in the global carbon cycle by taking up a significant fraction of the excess carbon dioxide that humans release into the atmosphere. As a consequence of humankind's collective release of CO_2 emissions into the atmosphere from fossil fuel burning, cement production, and land use changes over the last two-and-a-half centuries, commonly referred to as "anthropogenic CO_2" (C_{anth}) emissions, the atmospheric CO_2 concentration has risen from pre-industrial levels of about 278 ppm (parts per million) to ~410 ppm in 2019. The atmospheric concentration of CO_2 is now 47% higher than preindustrial levels (Friedlingstein et al. 2019). As discussed in previous *State of the Climate* reports, marine C_{anth} is the major cause of anthropogenic ocean acidification. Here the discussion is updated to include recent estimates of the ocean C_{anth} sink. Over the last decade the global ocean has continued to take up a substantial fraction of the C_{anth} emissions and therefore is a major mediator of global climate change. Of the 11 (±0.9) Pg C yr^{-1} C_{anth} released during the period 2009–18, about 2.5 (±0.6) Pg C yr^{-1} (23%) accumulated in the ocean, 3.2 (±0.6) Pg C yr^{-1} (29%) accumulated on land, and 4.9 (±0.1) Pg C yr^{-1} (44%) remained in the atmosphere with an imbalance of 0.4 Pg C yr^{-1} (4%; Fig. 2 of Friedlingstein et al. 2019). This decadal ocean carbon uptake estimate is a consensus view from a combination of measured decadal CO_2 inventory changes, models, and global air–sea CO_2 flux estimates based on surface ocean partial pressure of CO_2 (pCO_2) measurements from ships and moorings. Using ocean circulation models that include biogeochemical parameterizations and inverse models that are validated against or fit to observed air–sea exchange fluxes and basin-scale ocean inventories, Friedlingstein et al. (2019) showed that the oceanic anthropogenic carbon sink has grown from 1.0 (±0.6) Pg C yr^{-1} in the decade of the 1960s to 2.6 (±0.6) Pg C yr^{-1} in 2018. Riverine contributions supply an additional 0.45 to 0.78 Pg C yr^{-1} of natural carbon to the ocean.

2) Air–sea carbon dioxide fluxes

Ocean uptake of CO_2 is estimated from the net air–sea CO_2 flux derived from the bulk flux formula with air–sea differences in CO_2 partial pressure (ΔpCO_2) and gas transfer coefficients as input. Gas transfer is parameterized with wind as described in Wanninkhof (2014). This provides a net flux estimate. To determine the C_{anth} fluxes into the ocean, several other processes need to be taken into account. A steady contribution of carbon from riverine runoff, originating from organic and inorganic detritus from land, recently revised upward from 0.45 to 0.78 Pg C yr^{-1} (Resplandy et al. 2018) needs to be included. Other factors, such as natural carbon deposition into/onto the sea floor and margins and natural variations in the balance of CO_2 between the atmosphere and ocean, are assumed to be small. C_{anth} is therefore defined as the sum of the net flux and the riverine contribution. The data sources for pCO_2 are annual updates of surface water pCO_2 observations from the Surface Ocean CO_2 Atlas (SOCAT) composed of mooring and ship-based observations (Bakker et al. 2016) and the Lamont-Doherty Earth Observatory (LDEO) database with ship-based observations (Takahashi et al. 2017). The increased observations and improved mapping techniques including neural network methods (Rödenbeck et al. 2015) provide annual global pCO_2 fields on a 1° latitude × 1° longitude grid at monthly time scales. This allows investigation of variability on sub-annual to decadal time scales.

The monthly 2019 ΔpCO_2 maps are based on the observation-trained neural network approach of Landschützer et al. (2013, 2014). The 2019 values are projections based on observed sea surface temperature (SST), sea surface salinity (SSS), satellite chlorophyll-*a*, and atmospheric CO_2 for 2019; climatological mixed layer depths (MLD); and a neural network approach for pCO_2 developed from the data from 1982 through January 2019. The 2019 estimate uses the monthly wind fields from 2018, but changes in winds over time have a small effect on annual global air–sea CO_2 fluxes (Wanninkhof and Triñanes 2017). The C_{anth} fluxes from 1982 to 2019 suggest a decreasing ocean sink in the first part of the record and a strong increase from 2001 onward that continued

unabated into 2019 with a 0.2 Pg C yr^{-1} increase from 2018 to the 2019 estimate (Fig. 3.26). The amplitude of seasonal variability is large (≈1 Pg C yr^{-1}) compared to the long-term trend with minimum uptake in the June–September timeframe. The C_{anth} air–sea flux of 3.2 Pg C yr^{-1} in 2019 is 33% more than the revised 1997–2017 average of 2.40 (±0.46) Pg C yr^{-1}.

The average fluxes in 2019 (Fig. 3.27a) show the characteristic pattern of effluxes (ocean-to-air fluxes) in the tropical regions, in coastal upwelling zones, and in the high-latitude Southern Ocean around 60°S. Coastal upwelling regions include the Arabian Sea, off the west coasts of North and South America, and the coast of Mauritania. The western Bering Sea in the northwest Pacific was a strong CO_2 source as well in 2019, particularly in the March–April timeframe. The region with the largest efflux is the upwelling region of the eastern equatorial Pacific. The regions of effluxes are significant CO_2 sources to the atmosphere. The primary uptake regions are in the subtropical and subpolar regions. The largest sinks are observed poleward of the sub-tropical fronts. The frontal positions determine the location of the maximum uptake. This position is farther south and weaker in the Pacific sector of the Southern Ocean compared to the other basins.

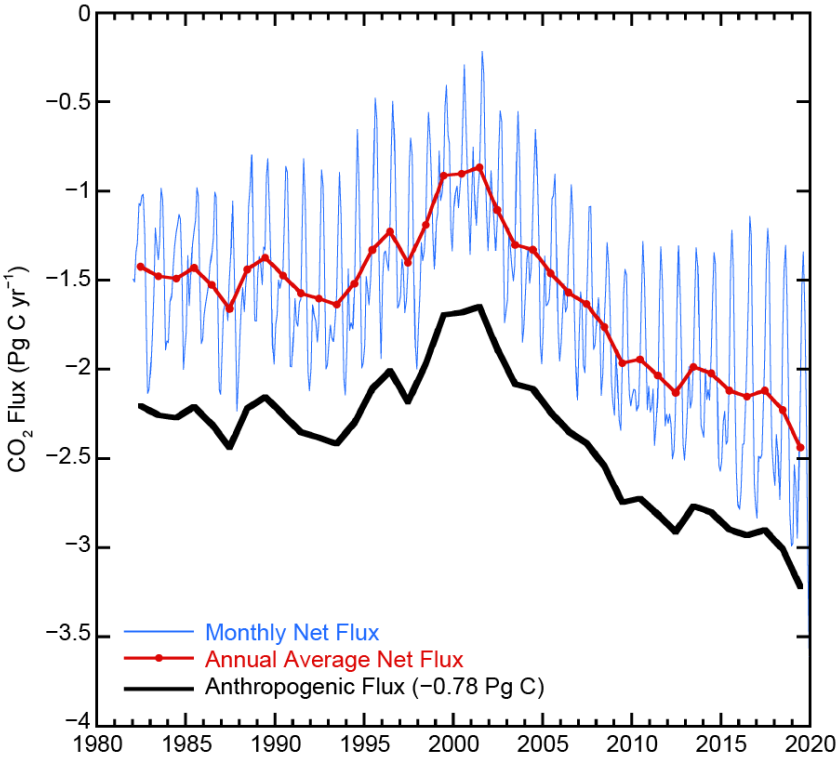

Fig. 3.26. Global annual (red line) and monthly (blue line) net CO_2 fluxes (Pg C yr^{-1}) for 1982–2019. The black line is the anthropogenic CO_2 flux that is the net flux plus the riverine component. Negative values indicate CO_2 uptake by the ocean.

In the Northern Hemisphere (NH), there is a significant asymmetry in fluxes in the sub-Arctic gyre, with the North Atlantic being a large sink while the North Pacific is a source of CO_2. This is, in part, due to the position of the western boundary currents that are known CO_2 sinks at high latitudes. The Gulf Stream/North Atlantic Drift in the Atlantic extends farther north than the Kuroshio in the Pacific.

Ocean carbon uptake anomalies (Fig. 3.27c) in 2019 relative to the 1997–2017 average are attributed to the increasing ocean CO_2 uptake with time (Fig. 3.26) and to variations in large-scale climate modes. The long-term air–sea flux trend since the minimum uptake in 2000 is 0.75 Pg C $decade^{-1}$, which leads to greater ocean CO_2 uptake (blue colors in Fig. 3.27a). Despite this trend, there are several large regions showing positive anomalies (efflux) for 2019, notably the eastern equatorial Pacific, the sub-polar Northwest Pacific (centered at ≈ 40°N), and the high-latitude Southern Ocean. The increased effluxes in the eastern equatorial Pacific are related to a mostly negative sign of the Oceanic Niño Index (ONI) that followed an extensive period of predominantly positive ONI (i.e., more El Niño-like) conditions in the preceding 20 years. The neutral sea surface temperature anomaly (SSTA; see Fig. 3.1a) indicates normal upwelling of waters with high CO_2 content has returned after a period of lower-than-normal upwelling. Positive anomalies (efflux) in the northwest Pacific regions, including the western Bering Sea, are related to the positive SSTA over the past year compared to the long-term average (Fig. 3.27c).

The differences between the air–sea CO_2 fluxes in 2019 compared to 2018 (Fig. 3.27b) are relatively small compared to previous years with anomalies roughly in the same regions as the difference of 2019 from the 20-year average. This indicates that conditions in 2019 resemble conditions in 2018. The increase in CO_2 effluxes in the northwest Pacific from 2018 to 2019 are associated with increased temperature and associated increase in pCO_2 caused by the return of the marine heatwave in this area (see also Fig. SB3.1). The Southern Ocean (south of 40°S) shows a decreasing sink in the polar front region (≈50°S) and increasing source to the south for the Atlantic sector of the Southern Ocean compared to 2018. The correlations with SSTA (2019 minus 2018) are more nuanced. The large positive SSTAs in the northwest Pacific from 30° to 60°N are indicative of the warm water anomaly and associated positive CO_2 flux anomaly (efflux; Fig. 3.27b). The large negative CO_2 flux anomaly (uptake) in the southeastern Pacific has a positive SSTA associated with it, and the positive flux anomaly around 45°S in the South Atlantic is associated with a negative SSTA. These flux differences are not readily explained in terms of SSTA and suggest that in this band, SSTAs and flux anomalies are decoupled. The North Atlantic near Greenland shows a large increase in sink strength with a positive SSTA that again cannot be readily explained in terms of local SSTA. Rather, it appears that changes in the ocean currents and biological productivity changes between 2019 and 2018 are the cause of the greater uptake.

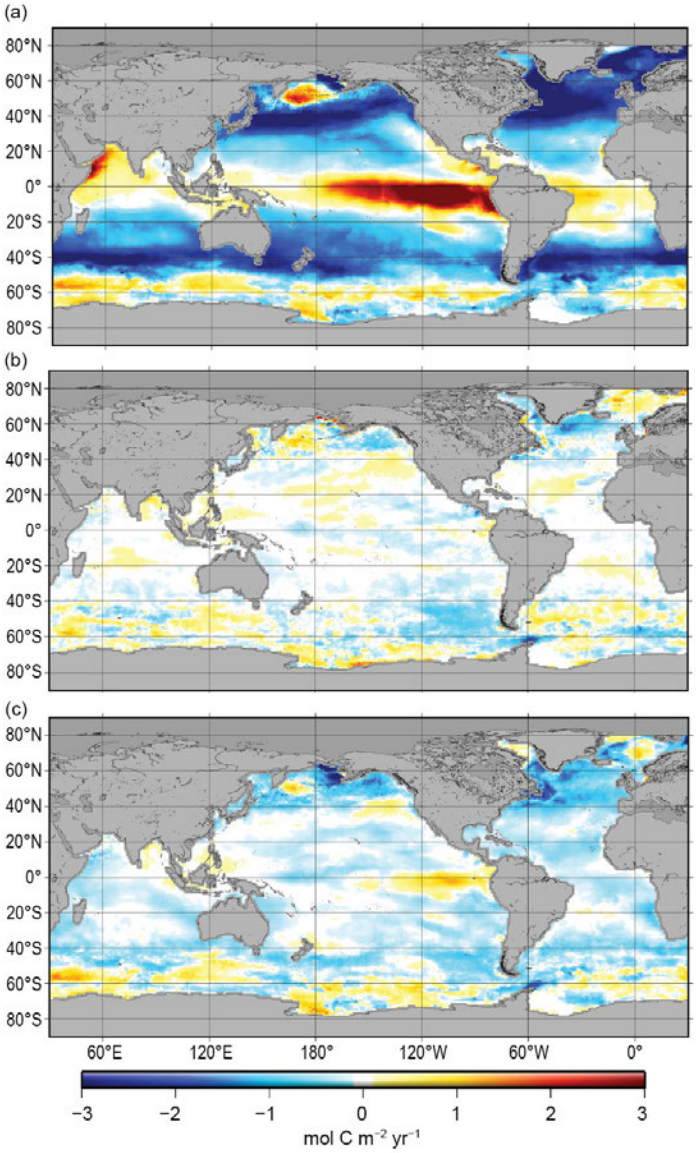

Fig. 3.27. Global map of (a) net air–sea CO_2 fluxes for 2019, with ocean CO_2 uptake regions shown in the blue colors, (b) net air–sea CO_2 flux anomalies for 2019 minus 2018 values following the method of Landschützer et al. (2013), and (c) net air–sea CO_2 flux anomalies for 2019 relative to a 1997–2017 average. All maps have units of mol C m^{-2} yr^{-1}.

Some of the pCO_2 and CO_2 flux anomalies can be attributed to variations in large-scale climate modes and associated physical anomalies, notably temperature, but the causality is often complex. For example, the behavior of pCO_2 with respect to temperature includes competing processes: thermodynamics dictate decreasing pCO_2 with decreasing SST, but waters originating from the deep with a cold temperature signal will have a high pCO_2. As the equilibration time of pCO_2 in surface seawater with atmospheric CO_2 is on the order of a year, CO_2 and CO_2 flux anomalies can be propagated by ocean currents. Moreover, the drawdown of pCO_2 due to biology is often associated with increasing temperature, but this depends on region and season. The strong trend of increasing CO_2 uptake since 2000–02 has continued through 2019, with an increase in 2019 of 0.2 Pg C yr^{-1} above the 2018 estimate. This increase meets the overall expectation that the ocean will remain an increasing sink if atmospheric CO_2 levels continue to rise. The sequestration of CO_2 by the ocean partially mitigates the atmospheric CO_2 rise but it comes at a cost of increased acidification of surface and subsurface waters (Feely et al., 2016; Carter et al. 2017; Lauvset et al. 2020).

3) Large-scale carbon and pH changes in the ocean interior

Global-scale CO_2 emissions from human activities are causing ocean interior C_{anth} increases and acidification. These large-scale changes can affect marine organisms and impact fisheries with implications for food security (Gattuso et al. 2015). Delineating how the biogeochemical processes in the ocean interior will be affected by the changing heat content and C_{anth} uptake is essential for developing future mitigation and adaptation responses to climate change. A major aim of the international Global Oceans Ship-based Investigations Program (GO-SHIP) is to determine the C_{anth} input to the ocean interior and the changing patterns of oceanic CO_2 over time (Talley et al. 2016; Sloyan et al. 2019). Field observations and inverse models have provided estimates of the uptake of C_{anth} into the ocean both over the last 250 years and over the last two decades. Simulations of C_{anth} inventories with models suggest that the ocean accumulated 24–34 Pg of C_{anth} between 1994 and 2007 (Gruber et al. 2019; Fig. 3.28a), accounting for about 25% of the total anthropogenic CO_2 emissions over that time period. This uptake has increased the total inventory of C_{anth} since 1750 from 118 ± 20 Pg C in 1994 to 170 ± 20 Pg C in 2018 (Sabine et al. 2004; Friedlingstein et al. 2019). Change in C_{anth} storage is determined by the change in C_{anth} between repeat surveys. This approach utilizes several newly developed methods and procedures for determining C_{anth} from the often much larger changes in the natural carbon content due to changes in transport ventilation and remineralization (e.g., Woosley et al. 2016; Clement and Gruber 2018; Carter et al. 2017, 2019). The approaches have been extended to allow for estimation of global ocean C_{anth} as well as extrapolation into coastal regions (Feely et al. 2016). These approaches have indicated that significant variability at interannual and decadal time scales occurs in some regions, particularly in the tropics due to El Niño–Southern Oscillation (ENSO) forcing, and in the subtropics and high-latitude regions due to changing ventilation processes that can alter the globally integrated sink (Carter et al. 2017, 2019; Rödenbeck et al. 2015; Landschützer et al. 2016; DeVries et al. 2017; Friedlingstein et al. 2019).

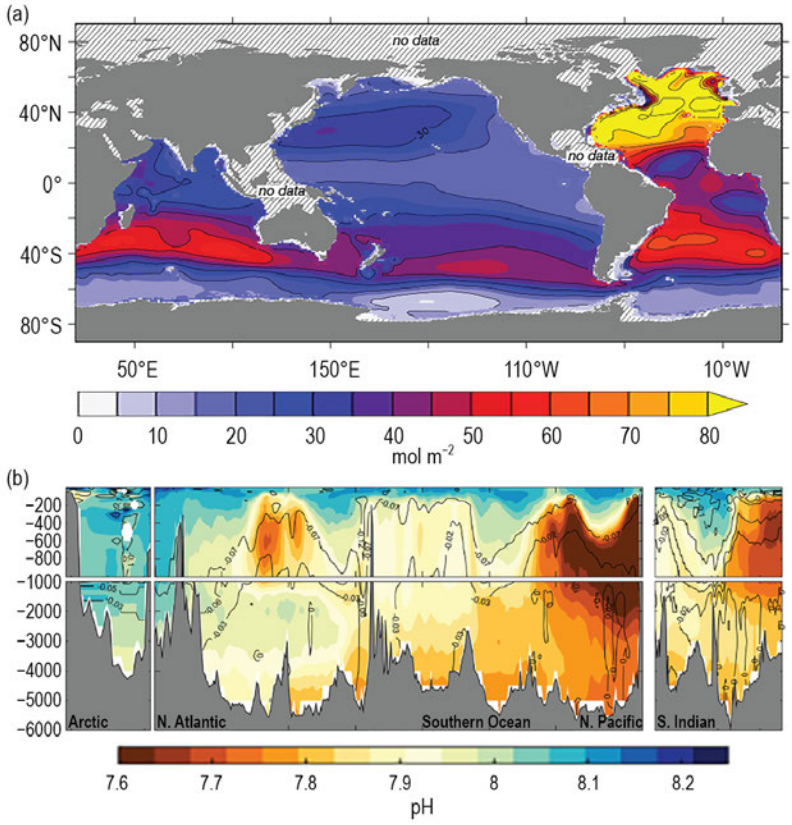

Fig. 3.28. (a) Change in full water column inventory of anthropogenic CO_2 in mol m^{-2} from 1994 to 2007, based largely on WOCE and GO-SHIP BGC data in the GLODAPv2 data product (modified from Gruber et al. 2019). (b) Vertical cross sections of pH (color) in the major ocean basins, from GO-SHIP transects from the Arctic (left) south through the Atlantic to the Southern Ocean (middle), then north through the Pacific along 152°W (middle, right) and north through the Indian Ocean along 85°E (right). The pH (total scale) is reported for in situ temperature and pressure and are normalized to year 2002 as in the GLODAPv2 data product (Lauvset et al. 2015). Anthropogenic change in pH from preindustrial to year 2002 is contoured (after Lauvset et al. 2020).

The GO-SHIP surveys have also been used to determine the long-term biogeochemical changes in carbonate chemistry including pH and calcium carbonate saturation state in the global oceans (Carter et al. 2017, 2019; Lauvset et al. 2015, 2020). From 1750 through 2018, surface ocean pH has declined by 0.018 ± 0.004 units $decade^{-1}$ in 70% of the ocean basins (Fig. 3.28b), and the surface aragonite saturation state has fallen by an average rate of 0.34% per year, causing more stress on carbonate mineral-forming organisms. The sensitivity of pH to changing atmospheric CO_2

concentration increases as temperature decreases. Hence the magnitude of ΔpH is largest in cold high-latitude waters. Anthropogenic changes in pH are amplified at depths where pH is naturally lower and dissolved inorganic carbon (DIC) is naturally higher, implying a larger change in pCO_2 and pH for a given change in DIC. As atmospheric CO_2 concentration increases, changes in the carbonate system and the individual carbonate system species will be directly affected with the changing buffer capacity of seawater (Feely et al. 2018). Continued observations and modeling studies are needed to determine how oceans keep pace with the atmospheric CO_2 increase.

Sidebar 3.2: **OceanObs'19** —S. CHIBA, M. DAI, T. LEE, E. LINDSTROM, N. ROME, S. SPEICH, M. VISBECK, AND W. YU

OceanObs: A thirty-year history

Every 10 years, the ocean-observing community convenes to evaluate opportunities for innovation and improved collaboration to sustain and enhance global observations of the ocean. The third, and most ambitious, community-driven conference—OceanObs'19—convened in Honolulu, Hawaii, on 16–20 September 2019. It brought together people from all over the world to communicate the decadal advances made in observing technologies and the remarkable science that observing networks have enabled—and to chart innovative solutions to society's growing needs for ocean information and ways in which collaborations can accelerate progress. The first OceanObs'99 conference, held October 1999 in Saint Raphaël, France, was a galvanizing force for ocean observations and climate. Ten years later, OceanObs'09, held September 2009 in Venice, Italy, moved the community toward a common vision for the acquisition of routine and sustained global information on the marine environment sufficient to meet society's needs for describing, understanding, and forecasting marine and climate variability and weather; sustainably managing living marine resources; and assessing longer-term trends.

OceanObs'19: An ocean of opportunity

OceanObs'19 assembled more than 1500 ocean scientists, engineers, and users of ocean observing technologies from 74 countries and across many disciplines. The community submitted 140 community white papers (CWPs) with over 2500 contributing authors. The conference goal was to improve governance of a global ocean observing system by improving advocacy, funding, and alignment with best practices, encompassed by the conference statement (www.oceanobs19.net/statement/) with the following key points:

1. Engage observers, data integrators, information providers, and users from the scientific, public, private, and policy sectors in the continuous process of planning, implementation and review of an integrated and effective ocean observing system;
2. Focus the ocean-observing system on addressing critical human needs, scientific understanding of the ocean and the linkages to the climate system, real-time ocean information services, and promotion of policies that sustain a healthy, biologically diverse, and resilient ocean ecosystem;
3. Harness the creativity of the academic research and engineering communities, and work in partnership with the private and public sectors to evolve sensors and platforms, better integrate observations, revolutionize information products about the ocean, increase efficiency, and reduce costs at each step of the ocean-observing value chain;
4. Advance the frontiers of ocean-observing capabilities from the coast to the deep ocean, all aspects of the marine biome, disease vectors, pollutants, and exchanges of energy, chemicals and biology at the boundaries between the ocean and air, seafloor, land, ice, freshwater, and human populated areas;
5. Improve the uptake of ocean data in models for understanding and forecasting of the Earth system;
6. Ensure that all elements of the observing system are interoperable and that data are managed wisely, guided by open data policies and that data are shared in a timely manner;